11TH INTERNATIONAL SYMPOSIUM ON PARTICLE IMAGE VELOCIMETRY – PIV15
Santa Barbara, California, September 14-16, 2015

Pixel-accurate dynamic masking and flow measurements around small breaststroke-swimmers using long-distance MicroPIV

F.G. Ergin[1], B. B. Watz[1] and N. Wadhwa[2]

[1] Dantec Dynamics A/S, Tonsbakken 16-18 Skovlunde, DK
Gokhan.Ergin@dantecdynamics.com

[2] Technical University of Denmark, Department of Physics and Center for Ocean Life, Kgs. Lyngby, DK

ABSTRACT

Microorganism locomotion is often the focus of biophysics studies, as these organisms move effectively through water, within the constraints of low Reynolds number locomotion. Optimal locomotion is required not only to conserve energy, but also to minimize flow disturbances to avoid detection by predators. In fact, some small organisms switch to a different swimming mode during growth, as a result of drastic morphological changes in their body. Several MicroPIV / PTV studies have been performed to quantify the flow fields and disturbances generated by the propulsion of small organisms. Recently the hydrodynamics of a ~220-µm-long Acartia tonsa nauplius were analyzed in Ref. 1 using time-resolved MicroPIV/PTV, where a two-step masking technique was applied to remove the organism from the particle images. In the current study, we use the same particle image ensemble but take a different approach for masking and velocimetry. The new three-step masking approach reveals two peaks in the swim velocity, each corresponding to one of the two power strokes. The organisms swim velocity results indicate that the nauplius is a periodic swimmer and a counter-rotating vortex system is observed during the power stroke indicating a toroidal vortex in three dimensions.

Keywords: Time-resolved MicroPIV, Long-distance MicroPIV, dynamic masking, bio-microfluidics

INTRODUCTION

Microorganisms are known to adapt different locomotion techniques based on their size and shape [1,2]. In fact, many microorganisms switch to a different swimming mode during their own lifecycle due to substantial morphological changes [1,3]. The main reason hypothesized for these transitions is the changing Reynolds number. At the intermediate Reynolds numbers experienced by many marine organisms such as copepods and mollusks, the viscous and the inertial forces have the same order of magnitude. As the organism grows, the inertial forces become more important compared to the viscous forces, and a need for a different swimming mode arises. The microorganisms find the most efficient locomotion technique for their size in order to conserve energy and minimize flow disturbances. There is also a strong motivation for research on biologically inspired micro-vehicles as there is a growing demand for micro vehicles moving in air and water for different purposes. Quantifying the hydrodynamics of the locomotion of small organisms can provide the much-needed input to develop micro scale robotic vehicles. Recently different parameters have been used to quantify the hydrodynamics and energetics of copepods [1,4,5]. These parameters include spatial and temporal decay of flow disturbance, energy dissipation, energy budget, and propulsion efficiency. These parameters require the accurate measurement of the flow field structure in a time resolved fashion. Time-resolved MicroPIV has great potential in quantifying flow fields around microorganisms in the realm of low Reynolds number locomotion.

Several MicroPIV / PTV studies have been performed to quantify the flow fields and disturbances generated by the propulsion of small organisms [1,6-9]. A few challenges still exist in such measurements: First of all, the object in question is most likely present in the flow field during the measurements. Since we are only interested in the flow field information, the successful removal (masking) of the object from the raw particle images is desired, without removing any useful information from the flow field. Second challenge is about the illumination. Most time-resolved MicroPIV systems use a

powerful, pulsed laser as illumination. This type of illumination can easily disable the organism or alter its normal locomotion behavior. A third challenge is related to repeatability of experiments to obtain reliable results. Performing measurements around biological objects means that there is very little control on the locomotion direction, and recapturing of certain dataset is extremely difficult, if not impossible. This requires very accurate PIV algorithms to calculate vector fields from single image pairs. A fourth challenge is related to the timing of the experiment; it is quite difficult to control when the microorganism will swim through the field of view. Therefore experiments often require special hardware with ring image buffers with post trigger functionality. Some of the challenges are addressed and these are explained in the following sections.

Figure 1 Schematic of *Acartia tonsa* nauplius during a power stroke [1].

EXPERIMENTAL SETUP

The experimental setup is described in Ref. 1 and is summarized here briefly: Copepods *Acartia Tonsa* were cultured at 18°C and before experiments they were transferred to the test aquarium containing filtered seawater. Only a few individuals were transferred in order to avoid possible interactions between them. The test aquarium is a glass cuvette (10x10x40mm) placed on a horizontal stage and kept at room temperature, between 18°C and 20°C. The measurement setup is a long-distance Micro Particle Image Velocimetry (LDμPIV) system in which the light sheet propagation direction and the camera viewing direction are perpendicular to each other. In biological flows, high-power visible laser illumination is often not preferred as this can disable the organism, or it can affect the normal locomotion behavior of the organism. For these reasons, a low-power, continuous-wave infrared laser (Oxford Lasers Ltd, 808nm wavelength) was used for illumination. Sheet forming optics was assembled to produce a 150μm thick light sheet, defining the measurement depth of the experiments. TiO_2 seeding particles smaller than 2μm were introduced in small quantities until a sufficient seeding density was achieved. The particle images were recorded on a high-speed CMOS detector (Phantom v210, Vision Research Inc.) at a frame rate of 2000 fps and at a resolution of 1280x800 pixels. The images were acquired with 11.65x magnification producing a 2.2 mm x 1.4mm field of view (FoV). Single frame image acquisition was performed using Davis software (LaVision GmbH, Göttingen, Germany) with a constant time difference of 500μs between frames. Since the FoV was only approximately $3mm^2$, the images were stored in a ring buffer and a manual trigger stopped the acquisition after the organism had passed through the FoV. Consecutive frames were analyzed for PIV processing - quite typical for time-resolved PIV measurements: 65 frames were analyzed to produce 64 flow field measurements. The first frame of the image ensemble is shown in Fig. 2, where a 0.2mm tall *Acartia Tonsa* is visible. From this instant on, *Acartia Tonsa* propels itself upwards through filtered seawater by pulling three breaststrokes, covering a distance of approximately 650μm (Average swim speed approx. 20mm/s). It is observed that *Acartia Tonsa* moves in an almost-vertical straight line and its angular orientation does not change significantly. Subsequent image analysis is performed using DynamicStudio (Dantec Dynamics, Skovlunde, Denmark) featuring Matlab link. This includes feature tracking, image masking, velocity field calculation, vector masking and phase-locked averaging.

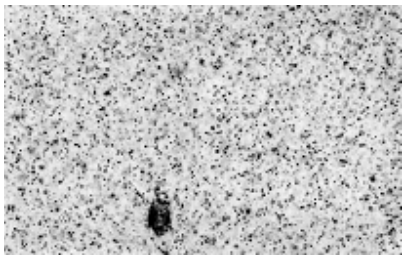

Figure 2 First frame of the raw particle image ensemble.

DYNAMIC MASKING

Objects and surfaces often appear in PIV images. Unless masked, these contribute to the cross correlation function and as a result introduce an uncertainty in the PIV calculation of the flow field. It is quite common and straightforward to use static masks to remove stationary objects, as these can be defined manually. However, it is not as trivial to mask moving objects or surfaces and literature on dynamic masking is quite limited. In practice, it is often possible to create dynamic masks of moving objects by applying a number of image processing functions to the original image ensemble. The idea behind dynamic masking is to get 0 pixel value on the object that is to be masked and retain the pixel value information everywhere else. This can be achieved in a two-step procedure. In step one, a new image ensemble is produced by filtering, thresholding etc. to obtain 0 pixel value on the object and 1 everywhere else. In step two, each time step of the new image ensemble is multiplied by the corresponding time step of the original ensemble. If the original image background pixel value is nonzero, this results in a sharp pixel value difference between the mask and the image background. As a remedy, background subtraction techniques can be used to obtain a 0 pixel value in the mask ensemble's background. Finally, the mask ensemble can be applied to mask either the raw images (image masking) and/or the PIV results (vector masking).

We tried several different dynamic masking strategies in a laboratory-fixed coordinate system, i.e. the real life situation where the fluid is stationary and the microorganism is in motion. These attempts produced unsuccessful results. Since the microorganism does not rotate around its axis, we decided to implement a simple tracking method and move to an object-fixed coordinate system, where the microorganism is fixed and the surrounding fluid is in motion. When the object is fixed in the frame conventional static masking techniques can be applied on the images and/or on the calculated vectors. This is achieved in three steps: First, a manual mask is generated using the organism's image in the first frame (Fig. 2), and this feature is tracked throughout the ensemble of 65 images. It was possible to define a constant feature that represents the organism because some of the seeding particles were stuck on the body and legs (Fig 3).

Figure 3 Close up of the *Acartia tonsa* showing particles stuck on its body.

The tracked feature was selected as the body of the organism excluding the legs, because the particles stuck on the body were stationary with respect to the organism and each other. Second, a pixel-accurate tracking algorithm was implemented as a Matlab script that locates the peak of the cross-correlation function between the defined feature and the entire image (Fig. 4). This essentially searches for the defined feature within the entire image. The algorithm is only pixel accurate because no subpixel fitting was performed during the computations. Third, when the organism location is established on all frames, a constant-size region of interest (ROI, 567x384 pix) around it is extracted. The vertical ROI dimension (384 pixels) is the maximum value that can be used in all the frames. The limitation is in fact the first and the last frames, where the distance fore and aft of the organism is defined. The horizontal ROI dimension (567 pixels) is a value that fixes the organism in the middle of the ROI horizontally and is sufficient to cover until the far field. This three-step procedure fixes the coordinate system on the organism, and allows the application of a conventional static mask to remove the organism (image masking) and eventually the spurious vectors on the organism (vector masking).

ADAPTIVE PIV PROCESSING

After masking of the organism, the particle displacements were computed using an Adaptive PIV algorithm with refinement steps, vector validation and deforming windows. The Adaptive PIV is an advanced and iterative cross-correlation based displacement estimator, where final interrogation windows of 16x16 pixel are used with 50% overlap. The vectors are considered valid if the peak height ratio is larger than 1.25. In other words, the displacement calculation is considered reliable when the highest peak (the assumed signal peak) is larger than 1.25 times the second highest peak

(assumed to be noise) in the cross-correlation function. This is certainly not the only vector validation method, but it is one of the oldest. A threshold value of 1.2 is often used in the literature, so in this respect our threshold value of 1.25 is more conservative. The subpixel positioning accuracy of the Adaptive PIV algorithm is reported as 0.055 pixels with 95% confidence [10]. This corresponds to a 94.4 nm displacement in the object space, and the velocity uncertainty is estimated as 189 µm/s, i.e. 1% compared to the average swim velocity.

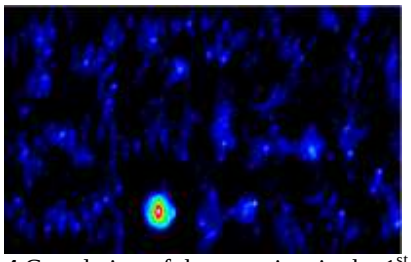

Figure 4 Correlation of the organism in the 1st frame.

RESULTS

The organisms swim velocity history can be measured by probing a vector in the far field, upstream of the organism, in a body-fixed reference frame. A time history of this vector shows that the nauplius is quite a periodic swimmer (Fig. 5), and that three full breaststroke cycles were recorded. One swim cycle period is measured as 10.5 ms (21 frames) and contains two forward breaststrokes followed by a recovery stroke. A careful investigation of the velocity time history reveals that there are two peaks during the power stroke, one corresponding to each breaststroke, followed by a full stop and a recess in the recovery stroke. The two peaks during the power stroke have not been observed previously and it is discovered in this study due to the superior quality of the tracking and dynamic masking process. The maximum swim velocity is recorded as 47.9 mm/s, during the second cycle during the second power stroke. These values are in good agreement with Ref. 1, where the maximum swim velocity values of 33.7 mm/s and 31.1 mm/s are reported. Additionally, a maximum reverse velocity is measured as 24.5 mm/s during the third cycle. In general, the magnitude of the maximum reverse velocity is approximately half the magnitude of the maximum forward velocity.

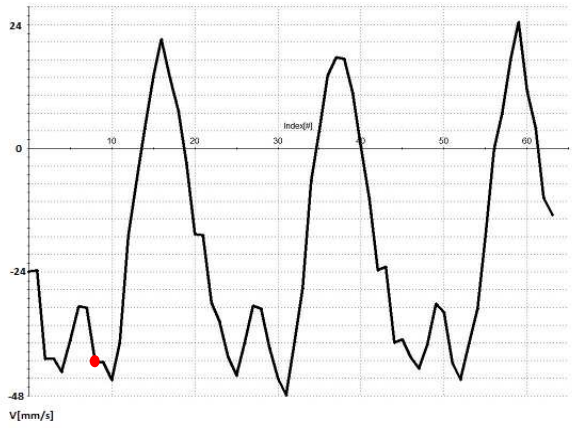

Figure 5 Time history of fluid velocity far upstream of the Nauplius in a body-fixed reference frame during 3 breaststrokes.

Finally, a phase-locked velocity averaging is performed over the three cycles and the instantaneous swim velocity value is subtracted to get the flow field details around the organism. Fig. 6 shows the flow field around the organism during the power stroke (at t=3.5 ms, frame index=8, corresponding to the red dot in Fig. 5) in the vicinity of the maximum swim speed. The colors indicate the magnitude of the velocity vector. In addition to the wake behind the organism, two vortices are observed; one on each side of the organism, with opposite rotation direction. The counter-rotating vortex system is an indication of toroidal (ring) vortex system in three-dimensions and is in agreement with the previous findings [1]. The observed toroidal vortex ring is cleaner in Fig. 6 when compared to Fig 2C and Fig. 2D in Ref 1. This is mainly due to the

phase-locked averaging of the flow field. Furthermore, the spatial dimension of the toroidal vortex is similar to the length of the organism.

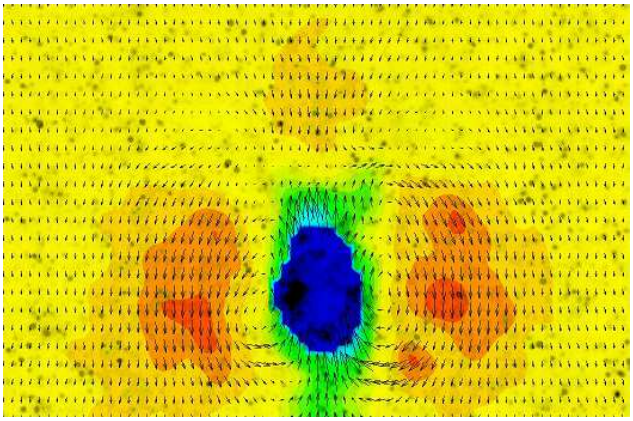

Figure 6 Flow field during power stroke (at the red point in Fig. 2a) Colors indicate velocity magnitude.

CONCLUSIONS & FUTURE WORK

Several important conclusions can be drawn from this experiment: Time-resolved long-distance MicroPIV is a powerful technique for investigation of flows around microorganisms if a suitable illumination source is used. Low-power infrared laser illumination proves to be an effective illumination mode, as it does not disable or affect the normal locomotion behavior of the organism. Furthermore, a new dynamic masking approach is used based on feature tracking. The importance of image pre-processing and dynamic masking must be stressed once again, as it can produce very different quality results for the same dataset. Using these, we were able to identify that *Acartia Tonsa* is a periodic swimmer, and discover the double velocity peak during the power stroke for the first time. The existence of the toroidal vortex is also reconfirmed. The maximum forward swim velocity magnitude was found approximately twice of the reverse swim velocity magnitude. Finally we can conclude that there is no single dynamic masking recipe that works globally. Dynamic masking strategies must be custom-made for each image ensemble. Future work includes the investigation of automatic post-triggering options to stop image acquisition in order to avoid long waiting times during the experiment. We also plan to conduct experiments around microscopic swimmers using a time-resolved Stereoscopic MicroPIV system for 2D3C measurements.

REFERENCES

[1] Wadhwa N, Andersen A and Kiørboe T "Hydrodynamics and energetics of jumping copepod nauplii and copepodids" *J. Exp. Biol.* (2014) **217**, 3085-3094

[2] Gustao JS, Rusconi R, and Stocker R "Fluid mechanics of planktonic microorganisms" *Ann. Rev. of Fluid Mech.* (2012) **44**, 373-400

[3] Childress S and Dudley R "Transition from ciliary to flapping mode in a swimming mollusc: flapping flight as a bifurcation in Re_{ω}" *J. Fluid Mech*. (2004) **498**, 257- 288

[4] Catton KB, Webster DR, Brown J and Yen J "Quantitative analysis of tethered and free-swimming copepodid flow fields" *J. Exp. Biol.* (2007) **210**, 299-310

[5] van Duren LA, Stamhuis EJ and Videler JJ "Copepod feeding currents: flow patterns, filtration rates and energetics" *J. Exp. Biol.* (2003) **206**, 255-267

[6] Pepper RE, Roper M, Ryu S, Matsudaira M and Stone HA "Nearby boundaries create eddies near microscopic filter feeders" J. R. Soc. Interface (2010) **7**, 851-862

[7] Roper M, Dayel MJ, Pepper RE and Koehl MAR “Cooperatively generated stresslet flows supply fresh fluid to multicellular choanoflagellate colonies” (2013) Phys. Rev. Lett. **110**, 228104

[8] Guasto JS, Johnson KA and Gollub JP “Oscillatory flows induced by microorganisms swimming in two dimensions” Phys. Rev. Lett. (2010) **105**, 168102

[9] Kiørboe T, Houshuo J, Goncalves RJ, Nielsen LT and Wadhwa N “Flow disturbances generated by feeding and swimming zooplankton” PNAS (2014) **111**, No. 32, 11738-11743

[10] Ergin FG, Watz BB, Erglis K and Cebers A “Time-resolved velocity measurements in a magnetic micromixer” Exp. Therm. Flu. Sci. (2015) **67**, 6-13